Brandeis University

Department of Physics

Senior Thesis

Networks of Coupled Chemical Oscillators

Author:
Matthew Carl Cambria

Principal Investigator:
Seth Fraden

May 1, 2015

Abstract

The oscillating Belousov-Zhabotinsky reaction (BZ) provides an experimental system with which to study networks of coupled oscillators. By emulsifying BZ in oil with surfactants, stable BZ drops will interact with each other through diffusion. Silicon microfluidics allow these drops to be arranged into custom planar networks with no-flux boundaries. The behavior of BZ drops in weighted star graphs is shown to depend upon two network variables, indicating that control over similar variables could be used to engineer the behavior of other networks of diffusively coupled oscillators.

Contents

List of Figures

List of Tables

1 Introduction

1.1 Motivations

There are numerous examples of both natural and artificial networks of coupled oscillators. Systems as diverse as the heart [1], a group of fireflies [2], and a power grid [3] can all be modeled as such networks. Despite their ubiquity, there are few experimental systems with which to study networks of coupled oscillators and those that do exist have numerous limitations. The oscillating Belousov-Zhabotinsky chemical reaction (BZ) provides a convenient system with which to study the networks that are the foundations of more complicated systems. In its own right, BZ is versatile, capable of oscillatory color change in solution and oscillatory volume change as a hydrogel [4]. By understanding the synchronization behavior of BZ networks, hydrogel volume changes could even be engineered into biologically inspired soft robots which could slither like a snake or beat like a heart.

1.2 BZ emulsion

Oscillatory reactions are both uncommon and counterintuitive. For these reasons, much research and writing has been done on the mechanism underlying the BZ reaction and multiple models have been proposed [5, 6, 7, 8]. In a homogeneous closed system at constant temperature and pressure the Gibbs free energy must decrease monotonically as a spontaneous chemical reaction progresses. This, however, does not prevent the oscillations of cer-

tain reactants. In BZ, the following overall reaction drives the free energy change that makes oscillations possible. In it, malonic acid is oxidized by bromate in acid.

$$3\,BrO_3^- + 5\,CH_2(COOH)_2 + 3\,H^+ \longrightarrow$$
$$3\,BrCH(COOH)_2 + 2\,HCOOH + 4\,CO_2 + 5\,H_2O \quad (O)$$

In the classic version of BZ which has cerium as its catalyst, reaction O is the result of two competing processes.

$$2\,Br^- + BrO_3^- + 3\,H^+ + 3\,CH_2(COOH)_2 \longrightarrow$$
$$3\,BrCH(COOH)_2 + 3\,H_2O \quad (A)$$

$$BrO_3^- + 4\,Ce(III) + CH_2(COOH)_2 + 5\,H^+ \longrightarrow$$
$$4\,Ce(IV) + BrCH(COOH)_2 + H_2O \quad (B)$$

Process A, during which the metal catalyst is in its reduced state, dominates above a critical bromide threshold. Process B, during which the metal catalyst is actively oxidized, dominates below this threshold. Oscillations occur because process A consumes bromide and process B indirectly produces it by the following two reactions.

$$6\,Ce(IV) + CH_2(COOH)_2 + 2\,H_2O \longrightarrow$$
$$6\,Ce(III) + HCOOH + CO_2 + 6\,H^+ \quad (B1)$$

$$4\,\mathrm{Ce(IV)} + \mathrm{BrCH(COOH)_2} + 2\,\mathrm{H_2O} \longrightarrow$$
$$4\,\mathrm{Ce(III)} + \mathrm{HCOOH} + 2\,\mathrm{CO_2} + 5\,\mathrm{H^+} + \mathrm{Br^-} \quad \text{(B2)}$$

By the time the concentration of bromide crosses the threshold and process A begins to dominate, reactions B1 and B2 will typically have reduced the Ce(IV) produced by process B. In the strain of BZ used in the following experiments, ferroin replaces cerium. Because the color of ferroin depends on its oxidation state, the color of BZ oscillates from red in the reduced state to blue in the oxidized state.

The synchronization behavior of microfluidically produced emulsions of BZ in oil has previously been studied in capillary tubes [9, 10]. Drops in such an emulsion are coupled by the diffusion of oil-soluble intermediate species, namely Br_2, $BrO_2\cdot$, and $HBrO_2$. The inhibitory species, Br_2, is produced as ferroin is oxidized during process B. In an emulsion, the bromine then diffuses from one drop to other which have lower bromine concentrations. The bromine delays oscillation because it is converted into bromide, prolonging process A. The other two species, $BrO_2\cdot$ and $HBrO_2$, are autocatalytic activators who promote oxidation which in turn produces more of them. Diffusion of these activators gives rise to traveling waves.

Malonic acid concentration has been previously used to control relative levels of inhibitory and excitatory coupling between drops in BZ emulsion [10]. In the following emulsion experiments, the malonic acid concentration allows inhibitory coupling to dominate. This suggests that the Vanag-Epstein

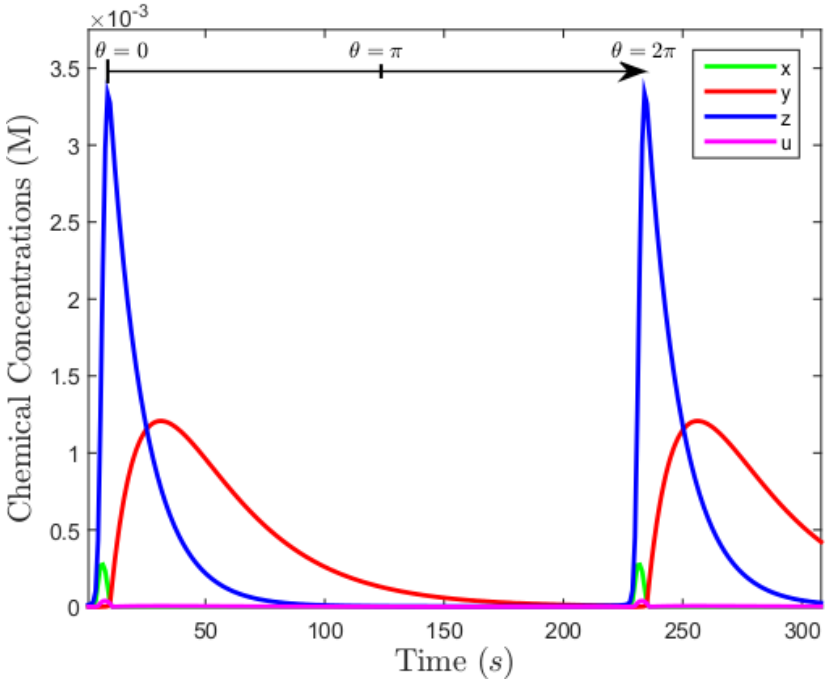

Figure 1: A simulated period of a BZ oscillator based on the four-variable Vanag-Epstein model A. Reactant z is the oxidized catalyst, which is responsible for the visible blue spikes in ferroin-catalyzed BZ.

model A (VE model) is applicable. By approximating the concentrations of some species involved in the reaction as steady-state, this model mathematically describes a single BZ oscillator with a tractable four variables.

$$dx/dt = -k_1xy + k_2y - 2k_3x^2 + k_4x(c_0 - z)/(c_0 - z + c_{min}) \quad (1)$$

$$dy/dt = -3k_1xy - 2k_2y - k_3x^2 + k_7u + k_9z \quad (2)$$

$$dz/dt = 2k_4x(c_0 - z)/(c_0 - z + c_min) - k_9z - k_10z \quad (3)$$

$$du/dt = 2k_1xy + k_2y + k_3x^2 \quad (4)$$

where $x = [\mathrm{HBrO_2}]$, $y = [\mathrm{Br^-}]$, $z = [\mathrm{Fe(phen)_3}^{3+}]$, and $u = [\mathrm{Br_2}]$. c_0 is

the total concentration of the catalyst and $c_{min}^2 = 2k_r(k_9 + k_10)c_0/k_{red}^2$.The various k_i are the rate constants of the reactions in the comprehensive Field-Kőrös-Noyes mechanism.

1.3 Reaction-Diffusion System

Networks of BZ emulsion can be mathematically described as a discrete reaction-diffusion system [11, 12]. In such a system, the concentration of a reactant can change within a drop, call it drop μ, in three ways: 1) the reactant may be consumed or generated by a chemical reaction within drop μ, 2) the reactant may diffuse between another drop and drop μ, or 3) the reactant may diffuse between the oil medium and drop μ. If the diffusive channels between drops are identical, then a discrete form of the reaction-diffusion equations can describe these three processes in a network of N drops and M reactants.

$$\frac{\partial \mathbf{x}^\mu}{\partial t} = \mathbf{D}\boldsymbol{\Delta}^\mu \mathbf{x}^\mu + \mathbf{F}_{\mathrm{x}}(\mathbf{x}^\mu), \qquad \mu = 1, ..., N \tag{5}$$

Here, $\mathbf{x}^\mu$ represents the concentrations of the M reactant in drop μ. $\mathbf{D}$ is a diagonal M by M matrix containing the coefficients of diffusive transport of each reactant. These coefficients, or coupling strengths, can be calculated from geometry, diffusion coefficients, and partition coefficients [12]. $\boldsymbol{\Delta}^\mu$ is the difference operator, defined as $\boldsymbol{\Delta}^\mu \mathbf{x}^\mu = \sum_\nu \mathbf{x}^\nu - \mathbf{x}^\mu$ where the index ν ranges over all the drops connected to drop μ. $\mathbf{F}_{\mathbf{x}}(\mathbf{x}^\mu)$ is, in general, a vector function describing reaction kinetics and diffusion into the continuous oil

phase of the emulsion. With a model of BZ such as the VE model, reaction-diffusion equations governing the system can be numerically solved for given boundary and initial conditions.

2 Methods

2.1 Microfluidic Emulsion Production

The BZ emulsion was produced using a PDMS-on-glass microfluidic chip. In order to keep the reaction from starting before the emulsion is produced, reactants are divided into two aqueous groups which are only mixed in the chip itself. The combined reactant stream is intersected by two perpendicular flows of oil which cuts the reactant stream into uniform drops. Flow rates are held constant by computer-controlled syringe pumps. The oil used was HFE-7500 (3M, St Paul, MN, USA) and to this was added 1.8% v/v of a fluorinated surfactant (EA, RainDance Technologies, Lexington, MA, USA) for drop stability. Drop size can be adjusted by varying the rates of reactant or oil flow, but for the experiments described here drops were 160 μm in diameter. The purpose of this small size is to allow each drop to be characterized by a single value at any moment. Larger unstirred oscillators exhibit traveling waves which prohibit this. The emulsion was collected in an Eppendorf tube.

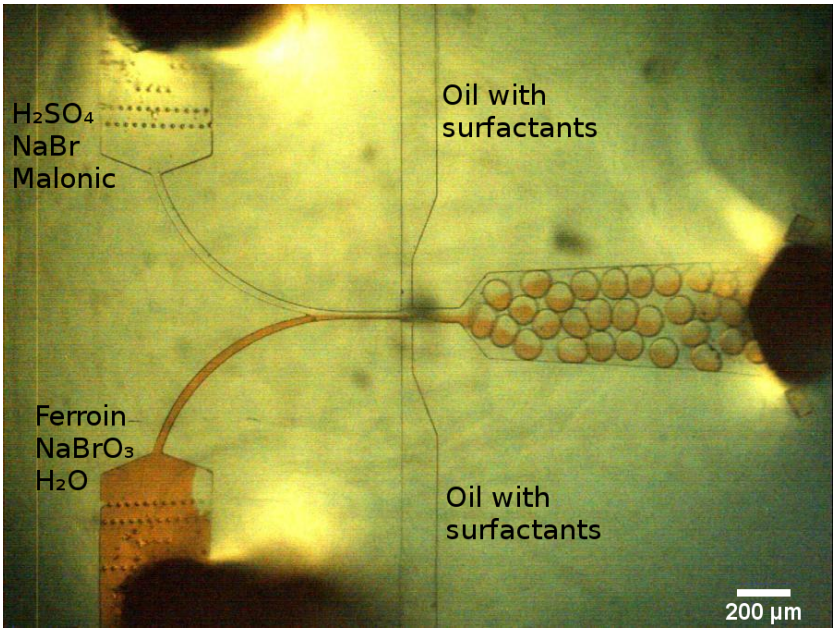

Figure 2: A still from a video of a microfluidic co-flow dropmaker in action. Two reactant streams mix before being cut into uniform drops by perpendicular flows of oil.

Reactant	Final Concentrations (mM)
Sulfuric acid (H_2SO_4)	60
Malonic acid ($CH_2(COOH)_2$)	400
Sodium bromide (NaBr)	10
Sodium bromate ($NaBrO_3$)	290
Ferroin ($Fe(phen)_3^{2+}$)	3

Table 1: Before mixing, concentrations were six times their values in the table. Equal parts of the first three reactants formed one reactant stream and the final two reactants were combined with one part water for the second reactant stream.

2.2 Silicon Microfluidics

The differential equations described in section 1.3 require boundary conditions to be set. The most desirable conditions for comparing experiment to theory are no-flux because these allow everything outside the system being studied to be ignored. Specifically, no-flux boundary conditions state that no species can cross the boundary of the system. Past experiments with BZ emulsion were done in capillaries or PDMS microfluidic chips, both of which had constant-chemical boundary conditions. In capillaries, there is no way to physically contain a geometry and so drops are necessarily diffusively interacting with all the drops in the tube, not just those of interest. Bromine is absorbed by PDMS so even though PDMS microfluidics allow for drops to be physically isolated, they do not provide chemical isolation.

In order to isolate custom geometries with no-flux boundary conditions, silicon microfluidic chips were developed. Using deep reactive ion etching (DRIE), custom designs were etched 70-80 microns into the surface of silicon wafers to produce microfluidic chips. The DRIE process begins with a silicon wafer to which a positive photoresist mask is photolithographically applied [13]. The wafer is placed inside the DRIE machine, which directs a beam of plasma that chemically etches any exposed silicon. Next a teflon-like passivation layer is applied to the surface of the waver. Another round of plasma is applied. The plasma sputters off the horizontal passivation layer, but leaves the vertical layers untouched because the plasma is directed perpendicular to the wafer's surface. The bottom of the silicon is thus exposed and susceptible

to the isotropic etch. The result of many applications of this cyclic process is an anisotropic etch, capable of producing nearly vertical walls. After etching the photoresist is removed from the wafer with acetone.

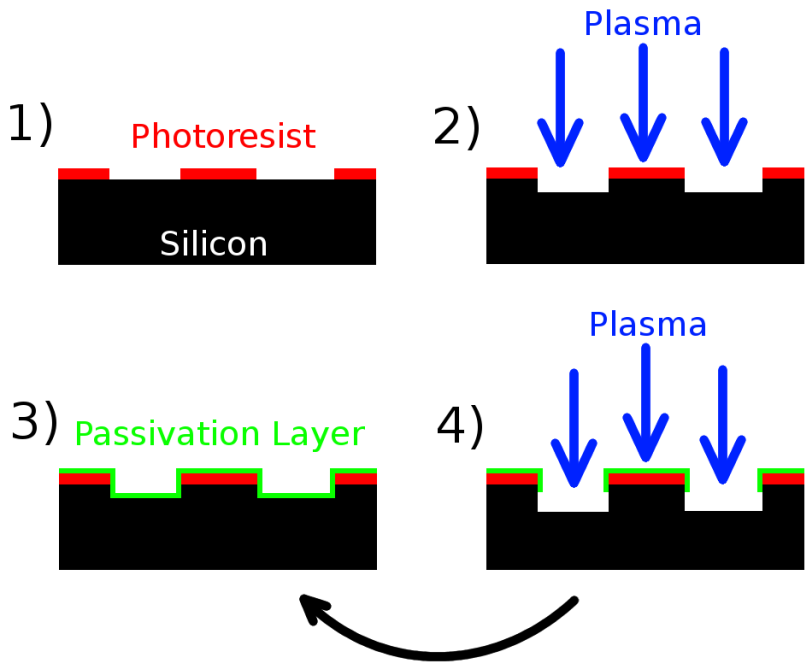

Figure 3: Deep reactive ion etching **1**) A side view of a silicon wafer with a photoresist mask. **2**) Directed plasma chemically reacts with the silicon surface, producing an isotropic etch. **3**) A passivation layer is applied to the exposed areas of the wafer. **4**) The plasma beam is again applied to the wafer. Because the beam is directed, it sputters off the bottom passivation layer but not the side layers. The silicon underneath is exposed and isotropically etched. The result of repeated applications of steps (3) and (4) is a highly anisotropic etch.

BZ drops were loaded into a silicon chip by first adding oil with surfactants (about $5\mu L/cm^2$) over the chip's features. This was the same oil with surfactants used to produce the drops. Next, a small amount of emulsion

(again, $5\mu L/cm^2$) was pipetted directly onto the features of the chip. Another round of oil with surfactants ($5\mu L/cm^2$) was added over the emulsion to spread the it. A clamp was then used to seal the chip with a glass microscope slide. Since BZ reactants diffuse through neither silicon nor glass, the glass-sealed silicon chips ideally provided the desired no-flux boundary conditions. In practice, there was a persistent layer of oil between the glass and the top of the silicon that the clamp could not diminish. It was assumed that the effects of this layer are negligible. After clamping, the droplets contained in the desired geometry were recorded through a microscope with a grayscale CCD camera. Images were collected at a frame rate of 1 frame every 10 seconds. Illumination was done by reflection with green light.

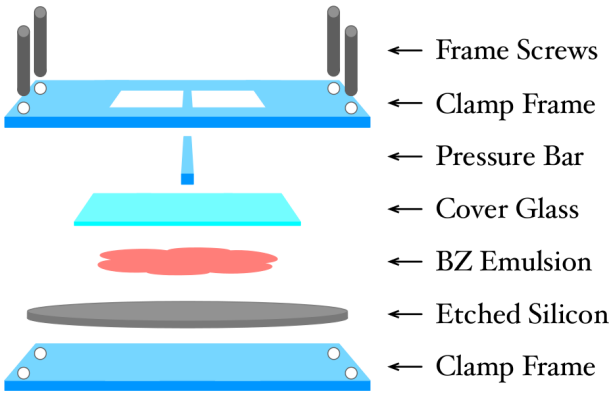

Figure 4: A diagram of the acrylic clamp used with silicon microfluidics. The emulsion is loaded directly on top of the silicon. A microscope slide is placed over the emulsion and the stack is placed into the clamp. The frame screws are tightened so that the pressure bar applies pressure the center of the microscope slide.

2.3 Star Graphs

Previous work has looked at one-dimensional arrays of drops in capillary tubes and rings of drops in microfluidic chips. Using silicon microfluidics, it is possible to look at more complex planar geometries, such as star graphs. A star graph, S_k, consists of a center node and k outer nodes, each of which is connected to the center node and no other nodes. The star graphs in the following experiments had k-fold radial symmetry. Two parameters of the star graphs were varied in order to look at their effect on drop behavior: 1) the degree k of the graph and 2) the distance between the center node and the outer nodes. This distance is defined by the length of the side of the straight channel connecting the inner and outer nodes.

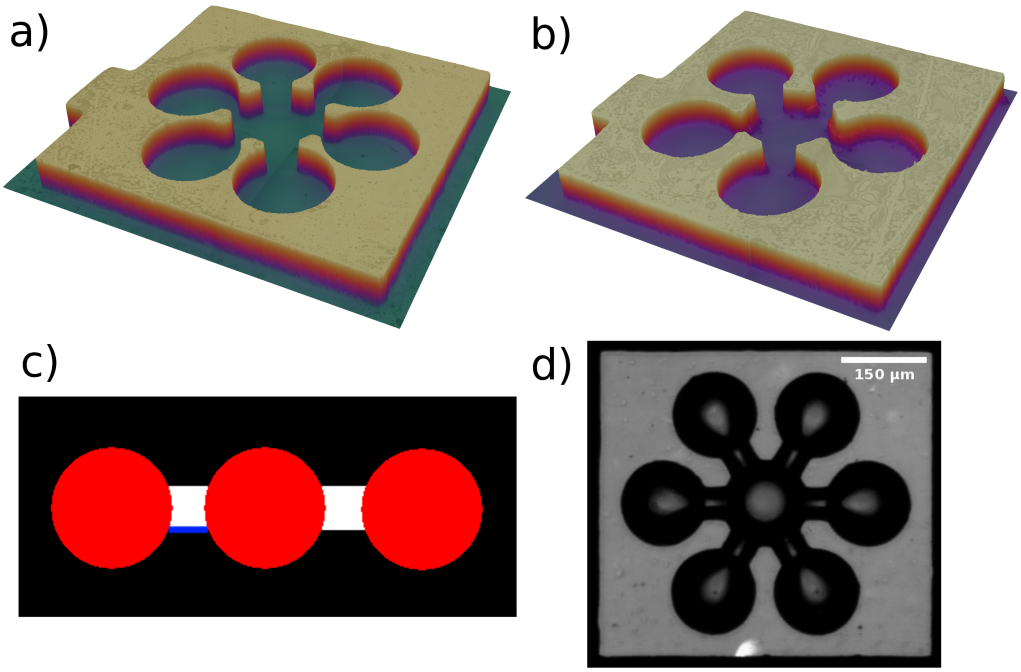

Figure 5: **a**) A three-dimensional, false color image of S_6 in silicon as viewed from an oblique angle. The coupling length is 20 microns. This image was produced with an optical profilometer. **b**) Another star graph in silicon, this time S_5 with a coupling length of 20 microns. **c**) A schematic of a star graph as viewed by the camera used in experiment. The red circles are BZ drops. The white regions are the coupling channels and the blue bar indicates where the coupling length is measured. The black is unetched silicon. **d**) S_6 in silicon with a coupling length of 50 microns as viewed by the camera. The network has been loaded according to the procedure described in the text.

2.4 Data Analysis

Data analysis was done with MATLAB. When the ferroin in a drop is oxidized, the color of the drop changes from red to blue and returns to red as the ferroin is reduced. Under the green illumination of the microscope, oxidized drops appear brighter than reduced drops. In order to assign a single intensity value to a drop in a frame, the image collected by the camera was first thresholded from grayscale to black-and-white based on a user-input threshold value. White areas of the image that could fit a circle of user-input size within them were morphologically opened by the same shape. The drop intensity was then defined as the average intensity of the pixels within this opening before thresholding.

Each drop was then defined a state based on this intensity value. If the drop's intensity in a frame t was a user-input value above the average intensity value of that drop over the ten previous frames, then the drop was defined to have spiked during that frame. A drop was only allowed to have spiked once during any ten frame interval so the spike indicates the first frame in which the drop was noticeably oxidized over the course of a single period. The duration of this period, $T_i(t)$, for a drop i at a time t was defined as the time between the next spike and the previous spike. The phase, $\phi_i(t)$, was assigned as a linear ascension from 0 to 2π:

$$\phi_i(t) = 2\pi \frac{t - t_{0i}}{T_i(t)} \tag{6}$$

where t_{0i} is the time of the last spike.

3 Results and Discussion

Data was collected for a range of star graphs with various combinations of the two parameters, star degree and coupling length. An order parameter was developed in order to characterize the behavior of a specific star graph. The order parameter distinguishes between three behaviors: 1) "locked", in which the difference between the phase of any outer drop and the inner drop is constant over time, 2) "unlocked", in which these phase differences are not constant, and 3) "center-silent", in which the center drop does not oscillate but the outer ones do.

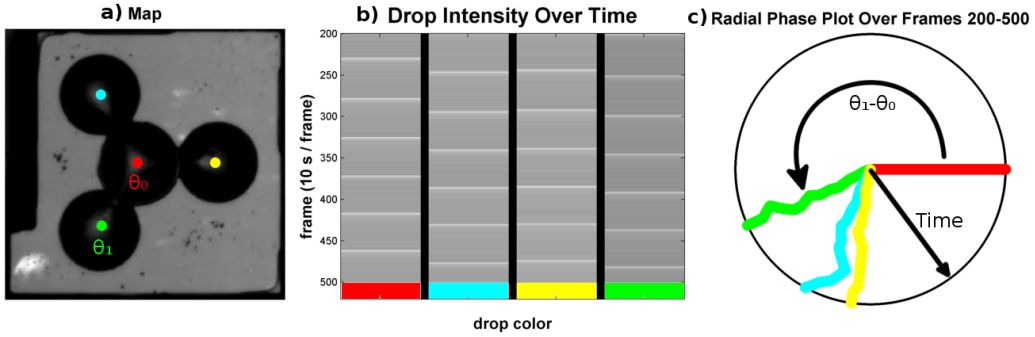

Figure 6: The locked behavior in a star graph with three outer nodes and a coupling length of 10 microns. **a**) A map of the graph indicating the position of the drops plotted in (b) and (c). **b**) The average intensity of a drop plotted as a grayscale color over frames 200-500. **c**) A radial phase plot. Each colored line traces the difference between the phase of a drop and that of the center drop. This phase difference is plotted as an angle which evolves radially in time. The colors indicate which drop is being compared to the center drop. The phase differences are "locked" at their respective angles, giving rise to the word describing the behavior.

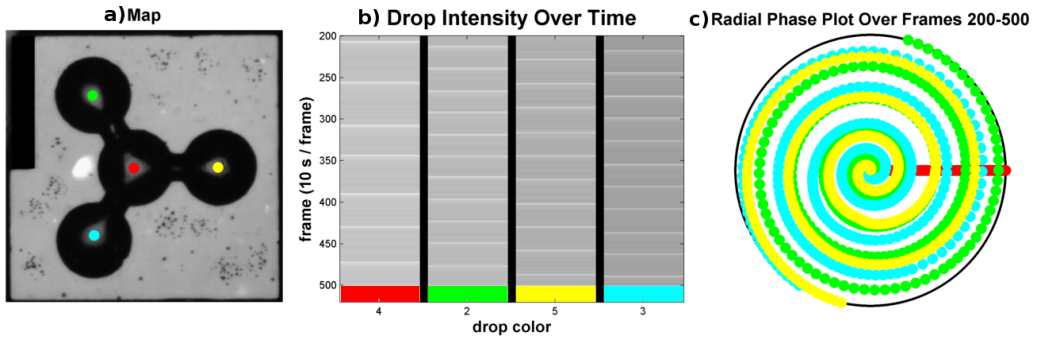

Figure 7: The unlocked behavior in a star graph with three outer nodes and a coupling length of 30 microns. **a**) A map of the graph. The period of the center drop is far slower than those of the outer drops. **b**) Drop intensity of frames 200-500. **c**) A radial phase plot. The phase differences are moving rapidly changing.

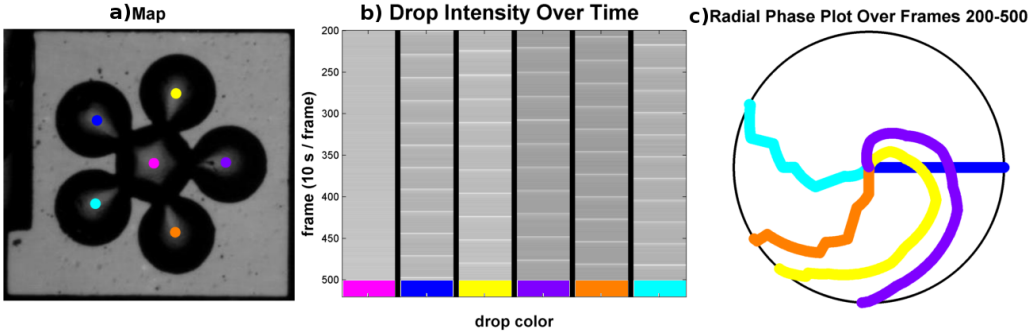

Figure 8: The center-silent behavior in a star graph with five outer nodes and a coupling length of 10 microns. **a**) A map of the graph. **b**) Drop intensity of frames 200-500. The center drop does not oscillate. **c**) A radial phase plot of phase differences relative to an outer drop, here the blue drop, instead of the center drop.

The first and second behaviors are defined by the derivative of the phase differences with respect to time. By equation 6, the phase difference between drops i and j at time t is given by

$$\phi_i(t) - \phi_j(t) = 2\pi\frac{t - t_{0i}}{T_i(t)} - 2\pi\frac{t - t_{0j}}{T_j(t)} \tag{7}$$

$$= 2\pi\left(\frac{1}{T_i(t)} - \frac{1}{T_j(t)}\right)t + 2\pi\left(\frac{t_{0j}}{T_j(t)} - \frac{t_{0i}}{T_i(t)}\right) \tag{8}$$

from which it is clear that

$$\frac{d}{dt}(\phi_i(t) - \phi_j(t)) = 2\pi\left(\frac{1}{T_i(t)} - \frac{1}{T_j(t)}\right) \tag{9}$$

So the essential distinction between locked and unlocked stars is the differences in the frequencies of the outer drops and the inner drop. This same information is carried by the differences in the periods and so these period differences were used in the final definition of the parameter.

For the order parameter to reflect the behavior of the entire star over a significant amount of time, the period differences between the outer drops and a reference drop, namely the center drop, must be averaged over number of drops and the selected frame interval. Averaging blindly, however, would give the same order parameter for some very different cases. Consider, for example, the order parameter that would result from averaging the period differences of the cyan drop and the orange drop, and the purple drop and the orange drop in figure 8. The purple drop is slower than the orange drop by approximately the same value that the cyan drop is faster than the orange

drop, so the average of the period differences would be near 0. The same value would arise if the three drops had identical periods. But these two scenarios describe the second and first behaviors, respectively, and so should not have the same order parameter. This problem is easily solved by looking instead at the absolute value of the period differences, which does not quantify how much faster or slower drops are with respect to the reference, but only the magnitude of the difference.

The order parameter can be cast into dimensionless form by dividing by the average period of a reference drop over the frame interval. Finally, the order parameter for a star of degree N with an oscillating center is

$$O_0 = \frac{1}{j-i+1}\frac{1}{N}\sum_{t=i}^{j}\sum_{k=1}^{N}\left|\frac{T_k(t)-T_0(t)}{\overline{T_0}}\right| \tag{10}$$

where k ranges over the indexes of the outer drops, i specifies the first frame in the selected interval, and j specifies the last. Drop 0 is the center drop. The order parameter can be made to accommodate a center-silent star by switching the reference from the center drop to some arbitrary outer drop.

$$O_1 = -\frac{1}{j-i+1}\frac{1}{N-1}\sum_{t=i}^{j}\sum_{k=2}^{N}\left|\frac{T_k(t)-T_1(t)}{\overline{T_1}}\right| \tag{11}$$

The negative sign distinguishes between the third behavior and the first two.

The values of i and j were chosen to be 200 and 500. The lower limit was set at 200 because it is assumed to be after initial transient behavior. The upper limit was set at 500 because it is before the graph is physically compromised by the gas generated by the reaction.

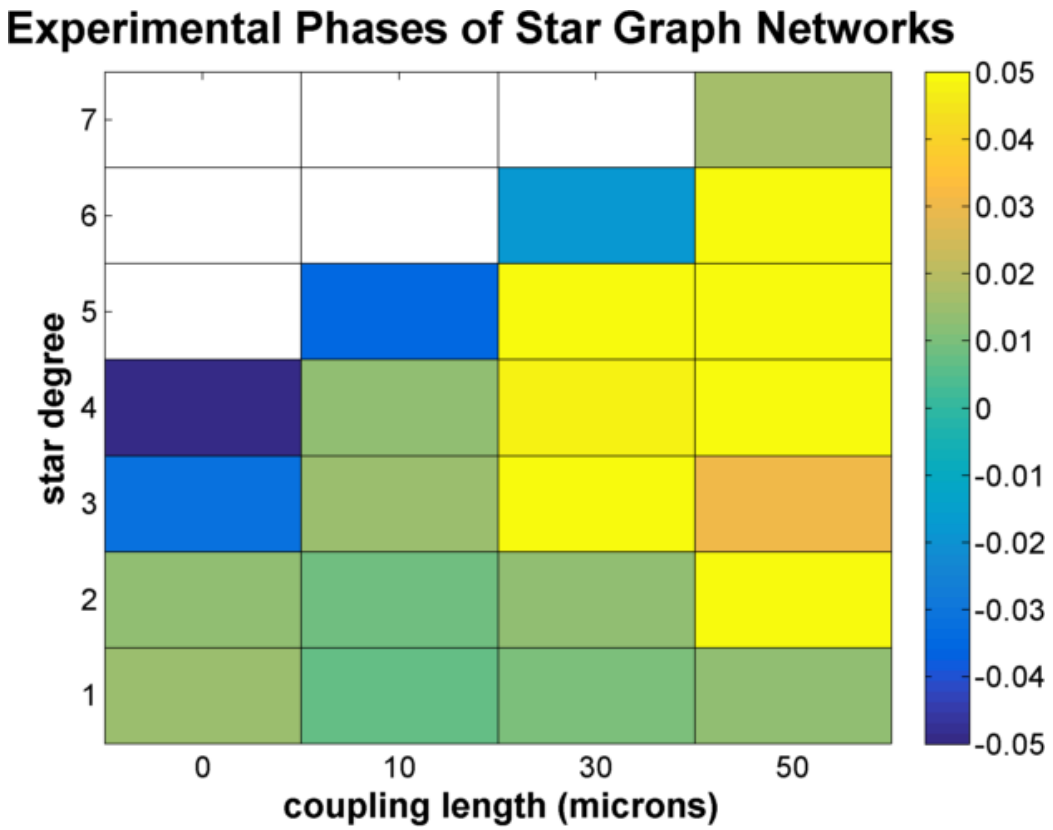

Figure 9: Order parameters of star graphs. The color indicates the value of the order parameter calculated for a star graph with coupling length and degree shown on the x and y axes respectively. White squares have no data because of geometrical limitations. The coupling between the outer drops and the inner drop increases towards the top left and decreases towards the bottom right. Values above and below the maximum and minimum values of the color bar are set to these values. Negative values are center-silent, low positive values are locked, and high positive values are unlocked.

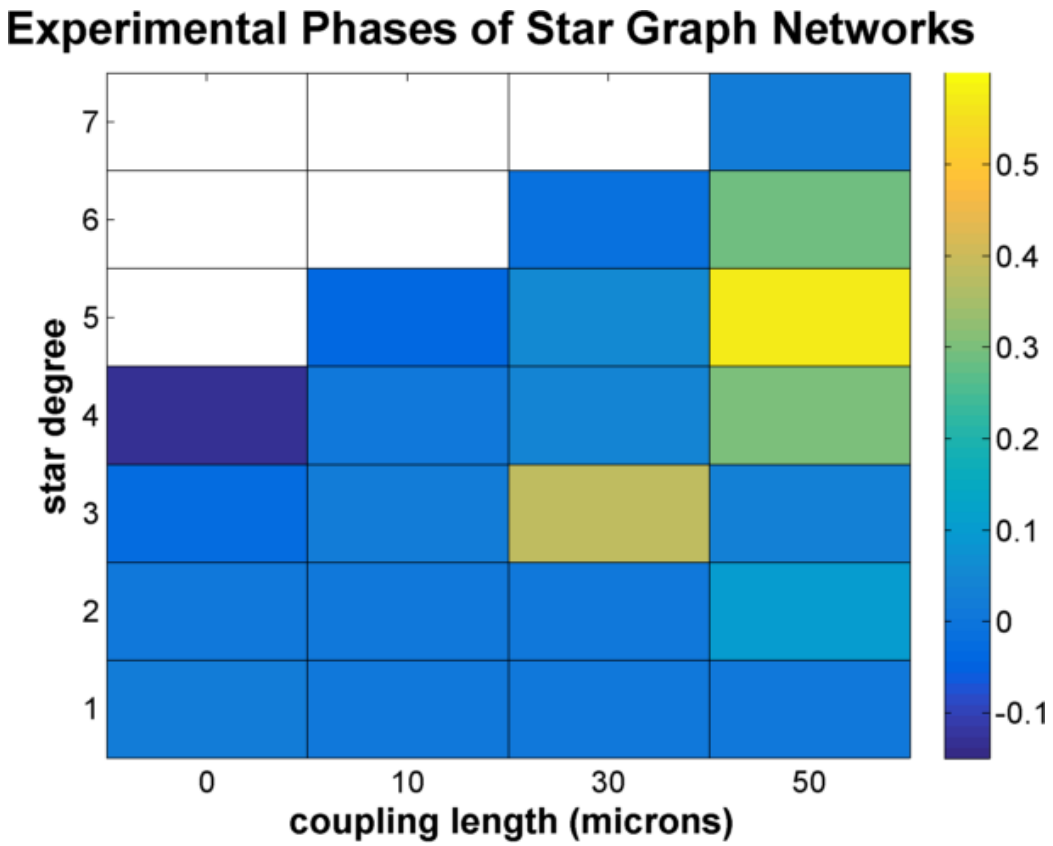

Figure 10: Order parameters of star graphs showing the details of the high and low values which were clipped in figure 9. Here the color bar is set so that there is no value outside its range. The high order parameters of some weakly coupled stars are due to period elongation of the center drop.

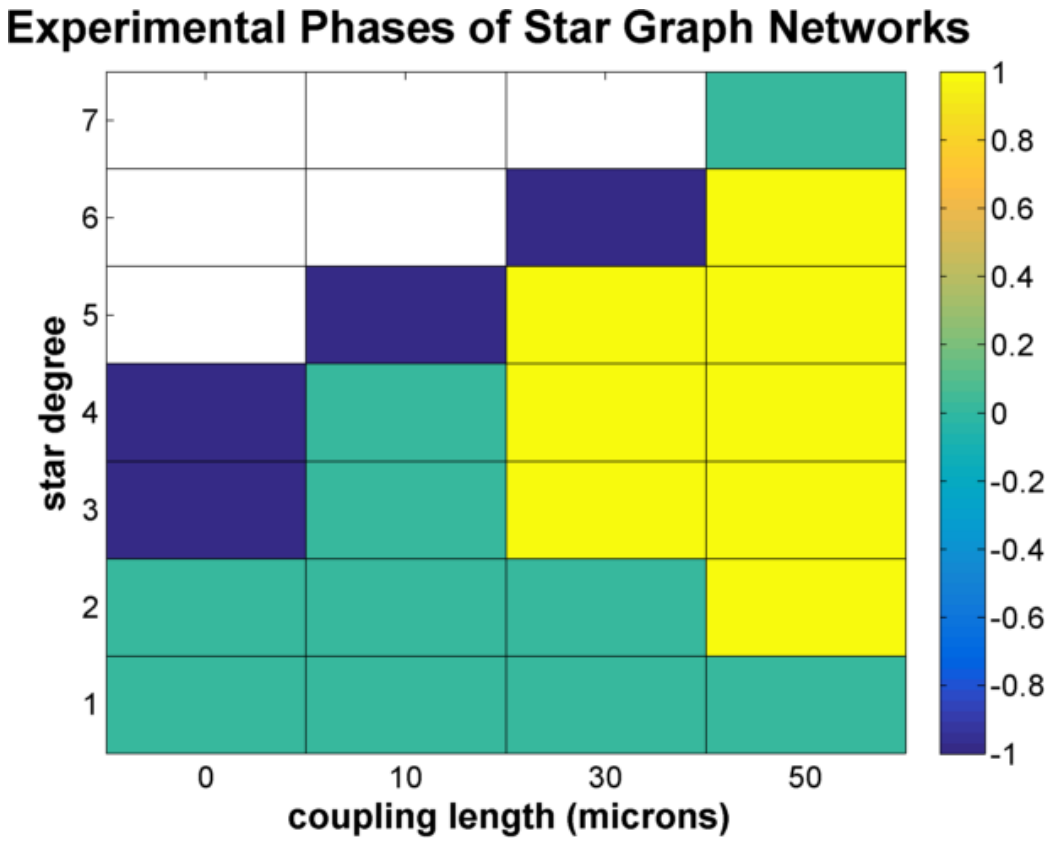

Figure 11: The same plot as in figures 9 and 10 but thresholded. Negative values were set to -1, values between 0 and 0.02 were set to 0, and values greater than .02 were set to one. Thus the three behaviors described are shown as discrete regions in the plot. The blue stars are center-silent, the green stars are locked, and the yellow stars are unlocked.

Coupling between the center drop and the outer drops increases as star degree increases and coupling length decreases. Figure 11 reveals three regions of behavior. Strongly coupled stars are center-silent, moderately coupled stars are locked, and weakly coupled stars are unlocked. The high order parameters of points in the weak coupling region are the result of elongated center drop periods, as can be seen in figure 7(b). The specific order parameters of center-silent stars are near those expected of a group of uncoupled drops which have some slight variation in period due to chemical heterogeneity. The origin of this heterogeneity is the dropmaker, which produces drops of nearly, but not exactly identical sizes and concentrations.

A positive order parameter of the same magnitude would be expected of a star with a very large coupling length. As the coupling increases from this very weak limit, the center drop is more strongly inhibited by the oscillations of the outer drops and so its period elongates. Interestingly, however, increasing the coupling further does not continue to elongate the center drop's period as might be expected. Instead, the period shortens to match the periods of the outer drops before it turns infinite in the strong coupling region.

4 Ongoing and Future Work

4.1 Star Graph Perturbations

By adding the light-sensitive catalyst $Ru(bpy)_3$ (rubipy) to the BZ chemistry, light can be used to stop oscillations [7]. Combining this with a pro-

grammable illumination microscope (PIM) allows for the selective suppression of certain drop's oscillations [9]. A PIM uses a standard projector with flipped optics to scale a projected image down in size. A specific drop can then be illuminated to suppress its oscillations while other drops are allowed to continue oscillating. In experiment, a star graph of degree five and gap length ten microns will have one outer member suppressed, effectively changing the star degree from five to four. With five outer members, this star is center-silent, but with four outer members it is locked. By turning off an outer member, it is hypothesized that the center drop's oscillations will revive. After the center begins oscillating, light suppression will be stopped, and the center droplet should stop oscillating once again. In a similar experiment, the center droplet of a locked star will be suppressed. Here, it is expected that the previously locked phases of the outer drops will begin to drift as the drops return to their natural frequencies. When the suppression of the center is stopped, the drops will again lock with the center.

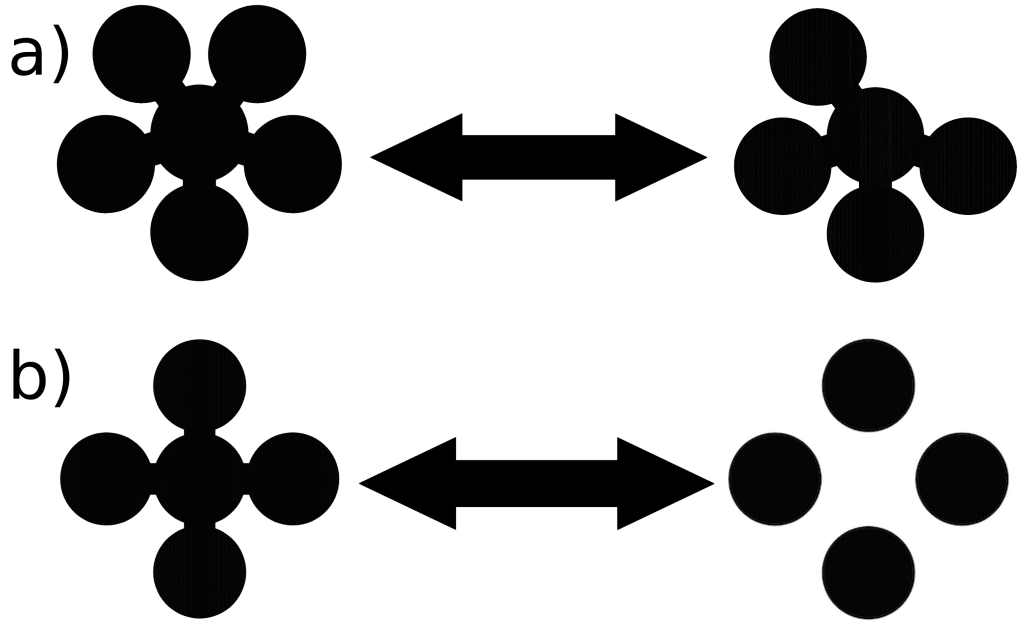

Figure 12: A representation of the star graph perturbation experiments. **a**) The first experiment described in the text. An outer member of a silent center star will be suppressed causing the revival of the center. Ceasing suppression of the outer member should cause the center to go silent once again. **b**) The second experiment described in the text. Suppressing the center of a locked star should cause the outer drops to oscillate at their natural frequencies. They should lock with the center once suppression is stopped.

4.2 Compartmentalized BZ in PDMS Microfluidics

In order to study a discrete rather than continuous BZ network, each oscillator in the network must have a nearly homogeneous concentration, otherwise the oscillator cannot be approximated as a single node in the network. Small quantities of BZ are used because diffusion occurs fast enough relative to the rate of reaction to validate the homogeneous approximation. Larger volumes of BZ can be stirred to the same effect, but these larger

volumes can have unstable periods and few spikes before oscillations stop, even with stirring. Additionally, diffusive coupling is easily achieved with microfluidic experiments. The use of drops, however, is not necessary to reap the benefits of micro-scale BZ networks. Compartmentalized BZ, that is, continuous BZ solution contained by microfluidic chips, makes possible a wide variety of networks that cannot be implemented with emulsified BZ.

Traveling waves in BZ have long been observed and studied [8]. These waves propagate due to the production of autocatalytic activators that occurs when the catalyst is oxidized. They can be used to excitatorily couple BZ oscillators by connecting BZ-filled wells with BZ-filled channels. The width of the channel would ideally be negligible so that there is no bulk flow between oscillators. This way, the system can be considered as two oscillators rather than a single strangely-shaped one. By containing such a design in PDMS, the oscillators will also be inhibitorily coupled since Br_2, the inhibitor, is soluble in PDMS. The excitatory coupling would occur only through the BZ itself since the activators are not soluble in PDMS. By changing the ratio of PDMS to BZ in the design of a coupling channel, the ratio of inhibitory to excitatory coupling can be controlled.

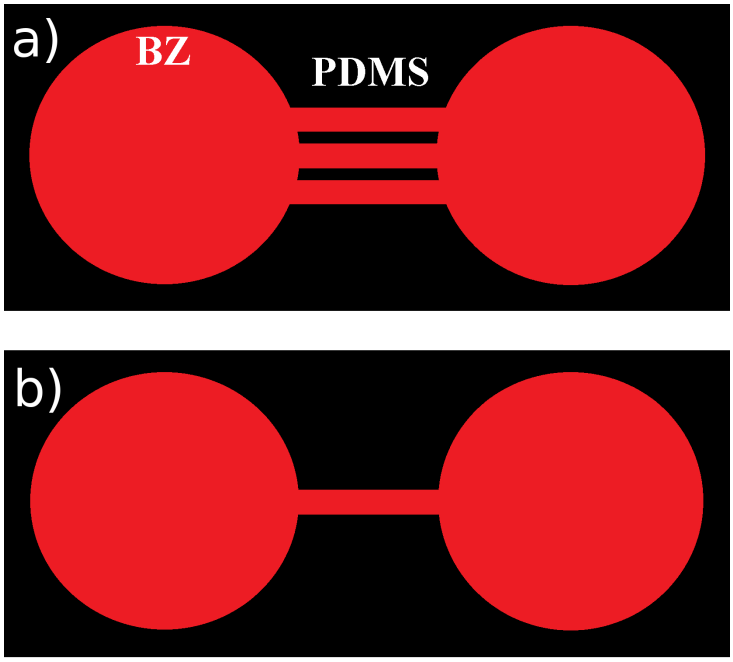

Figure 13: Two designs of two oscillators with different ratios of activatory to inhibitory coupling. **a**) The two red BZ wells are each oscillators. The oscillators are coupled by both BZ channels and their PDMS surroundings. **b**) There are fewer BZ channels connecting the oscillators so there is less activatory coupling between the oscillators here than there are in (a). Similarly, there is more inhibitory coupling since there is a greater volume of PDMS between them.

In typical thick PDMS microfluidic devices such as the dropmaker, the features of a design are empty spaces between glass and a thick layer of PDMS. Thick PDMS, however, absorbs bromine, rendering microfluidics of this sort useless for studying BZ. This can be overcome by thinning the layer of PDMS down to its absolute minimum by replacing the thick layer of PDMS opposite the glass with another piece of glass. This way, there is very little PDMS to absorb the bromine that the reaction requires.

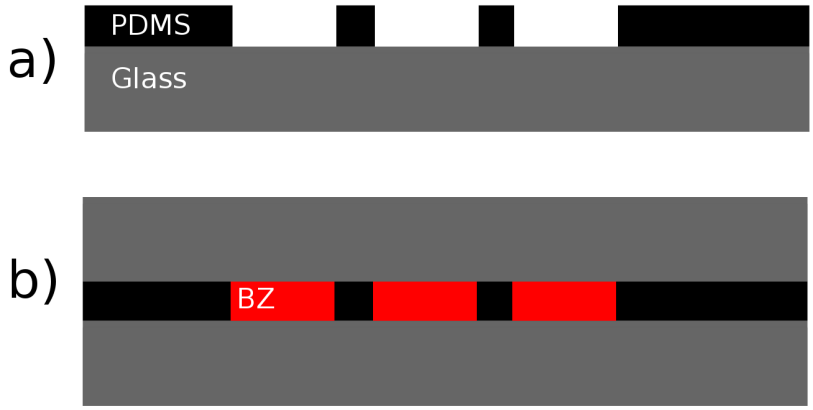

Figure 14: **a**) A side view of a thin PDMS microfluidic device. The typical thick layer of PDMS above the features is absent. Ideally, the designed layer of PDMS would be only as thick as the wells are deep. **b**) The same device loaded with BZ. BZ would be added directly on top of the PDMS and forced from between the PDMS and the top glass by clamping. The wells seen here would be excitatorily isolated from their neighbors.

Early tests have been done of the microfluidics described in figure 14, and both excitatory coupling and successful compartmentalization are evidenced. In figure 15, excitatory coupling is manifest in the top right corner of the frame as the oscillators are in phase. In the middle of the frame, drops oscillate with no apparent phase relationship indicating there is less excitatory coupling. This is likely due to the clamping failure described in figure 16. Ideally all of the top surface of the PDMS would be in contact with the glass, but this has proven difficult to accomplish. Gaps between this surface and the glass couple excitatorily oscillators with an undesired thin layer of BZ. Solutions to this problem are currently being investigated.

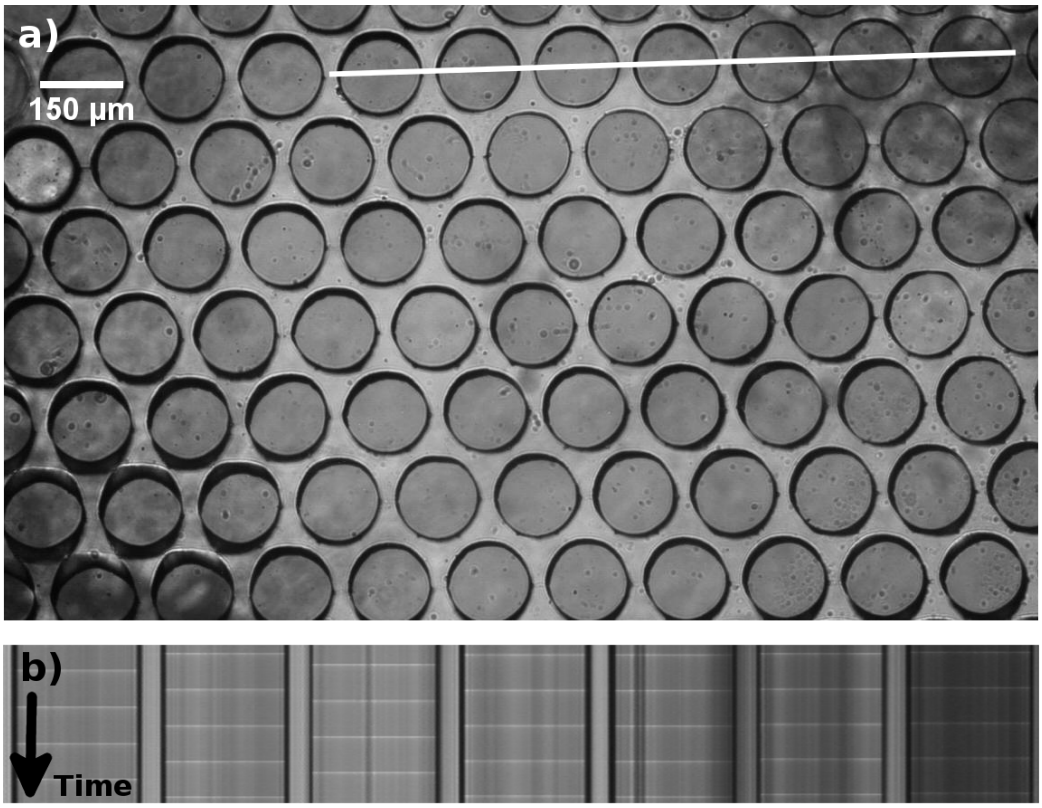

Figure 15: **a**) A thin PDMS microfluidic chip loaded with continuous BZ and sealed with a microscope slide. The dark circles are BZ-filled wells. The area around them is PDMS. **b**) A spacetime plot taken over 150 frames. Each horizontal line of pixels is a reproduction of the pixels at the white line in (a) at the time designated by the vertical axis. The first line is from the first frame, the second line is from the second frame, and so on. The four oscillators on the right are in phase, while the three on the left are not.

Figure 16: The in-phase oscillations seen in figure 15 were likely caused by a "short circuit" in which ineffective sealing allowed a thin layer of BZ to between the PDMS and the glass to excitatorily couple neighboring oscillators.

5 Conclusion

It has been shown that the behavior of networks of drops of the oscillatory Belousov-Zhabotinsky reaction depends on parameters of those networks. The counterintuitive non-monotonic dependence of the period of a star graph's center drop on those parameters has been described and further experiments with networks of BZ have been proposed. Ultimately, it is hoped that an understanding of networks of coupled BZ oscillators can illuminate the workings of other networks of coupled oscillators and lead to BZ technologies that make use of geometrically engineered behaviors.

References

[1] J. Honerkamp. The heart as a system of coupled nonlinear oscillators. *Journal of Mathematical Biology*, 18:69–88, 1983.

[2] B. Ermentrout. An adaptive model for synchrony in the firefly pteroptyx malaccae. *Journal of Mathematical Biology*, 29:571–585, 1991.

[3] Duncan J. Watts and Steven H. Strogatz. Collective dynamics of 'small-world' networks. *Nature*, 393:440–442, 1998.

[4] Ye Zhang, Ning Zhou, Ning Li, Megan Sun, Dongshin Kim, Seth Fraden, Irving R. Epstein, and Bing Xu. Giant volume change of active gels under continuous flow. *Journal of the American Chemical Society*, 136:7341–7347, 2014.

[5] Richard J. Field, Endre Körös, and Richard M. Noyes. Oscillations in chemical systems. ii. thorough analysis of temporal oscillation in the bromate-cerium-malonic acid system. *Journal of the American Chemical Society*, 94:8649–8664, 1972.

[6] Richard J. Field and Richard M. Noyes. Oscillations in chemical systems. iv. limit cycle behavior in a model of a real chemical reaction. *The Journal of Chemical Physics*, 60:1877–1884, 1974.

[7] Vladimir K. Vanag and Irving R. Epstein. A model for jumping and bubble waves in the belousov-zhabotinsky aerosol ot system. *The Journal of Chemical Physics*, 131, 2009.

[8] Irving R. Epstein and John A. Pojman. *An Introduction to Nonlinear Chemical Dynamics*. Oxford University Press, 1998.

[9] Jorge Delgado, Ning Li, Marcin Leda, Hector O. González-Ochoa, Seth Fraden, and Irving R. Epstein. Coupled oscillations in a 1d emulsion of belousov–zhabotinsky droplets. *Soft Matter*, 7:3155–3167, 2011.

[10] Ning Li, Jorge Delgado, Hector O. González-Ochoa, Irving R. Epstein, and Seth Fraden. Combined excitatory and inhibitory coupling in a 1-d array of belousov–zhabotinsky droplets. *Physical Chemistry Chemical Physics*, 16:10965–10978, 2014.

[11] H. G. Othmer and L. E. Scriven. Instability and dynamic pattern in cellular networks. *Journal of Theoretical Biology*, 32:507–537, 1971.

[12] Nathan Tompkins, Ning Li, Camille Girabawe, Michael Heymann, G. Bard Ermentrout, Irving R. Epstein, and Seth Fraden. Testing turing's theory of morphogenesis in chemical cells. *Proceedings of the National Academy of Sciences*, 111:4397–4402, 2014.

[13] Franz Laermer and Andrea Schilp. Method of anisotropically etching silicon, 1996. US Patent 5,501,893.